Supplement of Atmos. Meas. Tech., 17, 1375–1401, 2024
https://doi.org/10.5194/amt-17-1375-2024-supplement

Atmospheric Measurement Techniques
Open Access
EGU

Supplement of

The importance of digital elevation model accuracy in X_{CO_2} retrievals: improving the Orbiting Carbon Observatory 2 Atmospheric Carbon Observations from Space version 11 retrieval product

Nicole Jacobs et al.

Correspondence to: Nicole Jacobs (n.jacobs@utoronto.ca)

S1 Number of OCO-2 v10 soundings used to extract OCODEM elevations

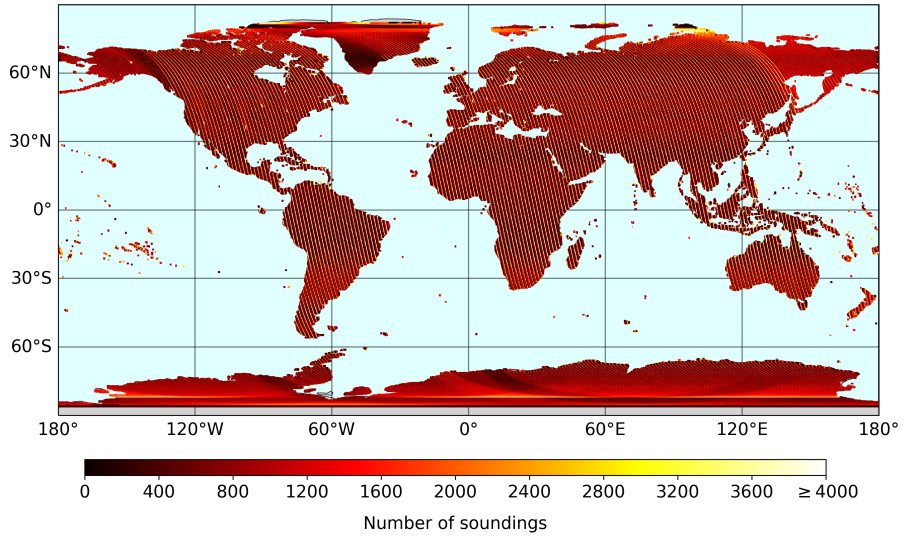

Figure S1. A map of the number of OCO-2 v10 soundings used to reconstruct the OCODEM at $0.1^\circ \times 0.1^\circ$ resolution from sounding altitudes. This map shows the striated pattern of regions with fewer soundings, most notable in the tropics and southern hemisphere, and this decreased coverage likely contributes to minor errors in the regridded OCODEM data used in this study.

S2 Maps of bias in OCO-2 retrieved surface pressures (dP)

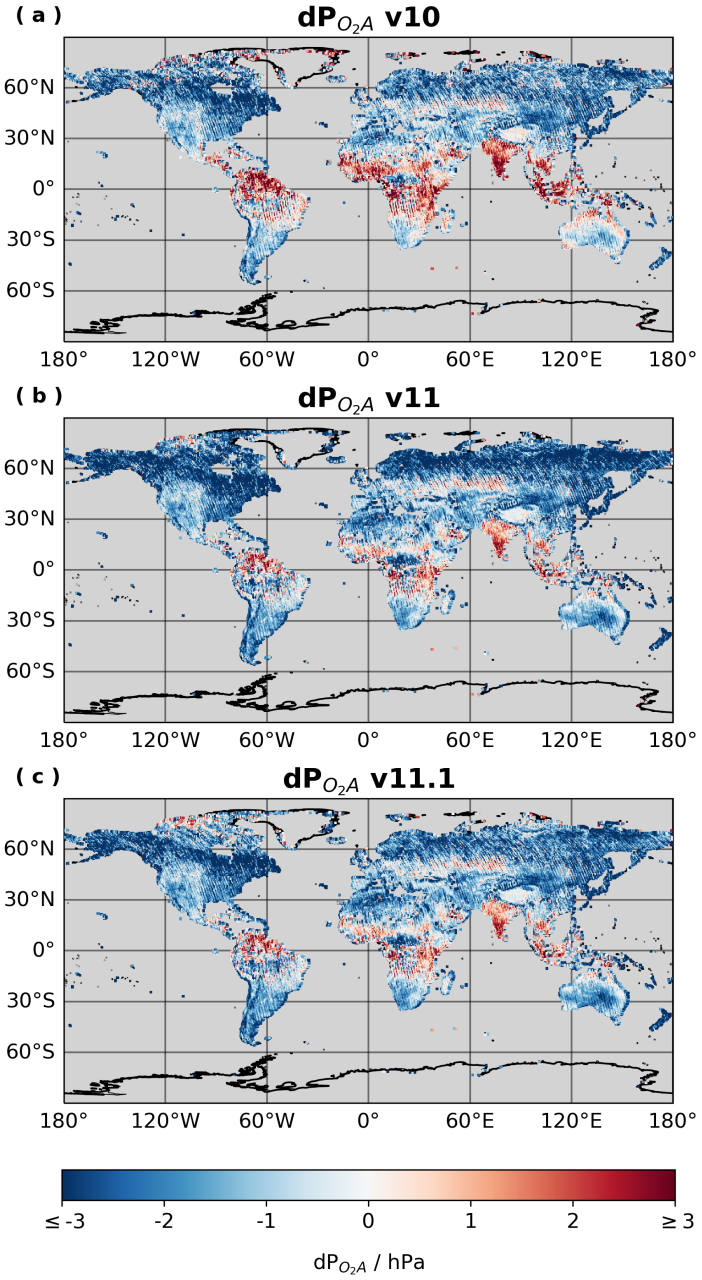

Figure S2. The mean dP (retrieved minus prior surface pressure) in the O_2A band for (a) all OCO-2 ACOS version 10 (v10) soundings, (b) all OCO-2 ACOS v11 soundings, and (c) all OCO-2 ACOS v11.1 soundings available in lite files, passing global quality controls in v10, v11, and v11.1, and aggregated to $0.5^\circ \times 0.5^\circ$ spatial resolution. Prior surface pressures are defined by GEOS-FPIT surface pressures hypsometrically adjusted to the surface elevation using a reference digital elevation model (DEM), which is the OCODEM for OCO-2 v10.

S3 Additional examples of target measurements over TCCON sites

S3.1 Pasadena

At Pasadena there are a relatively large number of OCO-2 target mode measurements with coincident TCCON observations and good spatial coverage for OCO-2 retrievals after quality control filtering. Overall, the changes in sounding altitudes across OCO-v2 v10 (OCODEM), v11 (NASADEM+), and v11.1 (Copernicus GLO-90) are small. In general, the mean bias in X_{CO_2}over Pasadena is reduced in v11.1, but the standard deviation in bias is similar to or slightly worse than that for v10 and v11. Figures S3 through S5 provide some examples throughout the year that illustrate these points.

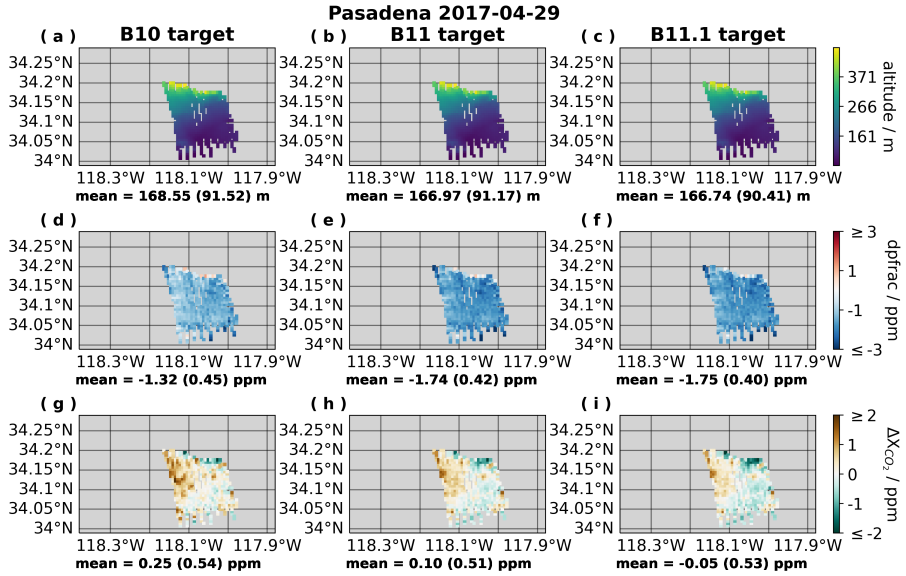

Figure S3. Sounding altitudes (top row; calculated for the sounding footprint as described in Sect. 3.1 and 3.2), retrieved dP$_{frac}$ (middle row), and OCO-2 bias in bias-corrected X$_{CO_2}$ relative to TCCON X_{CO_2} (see Sect. 3.3) (bottom row) during an OCO-2 target-mode overpass at Pasadena on 29 April 2017. Plots (a), (d), and (g) show results with OCO-2 v10 retrievals. Plots (b), (e), and (h) show results with OCO-2 v11 retrievals. Plots (c), (f), and (i) show results with the OCO-2 v11.1 retrievals. Only soundings that pass quality control filters in all three versions of the OCO-2 retrievals are included, such that the same set of soundings are included in all plots.

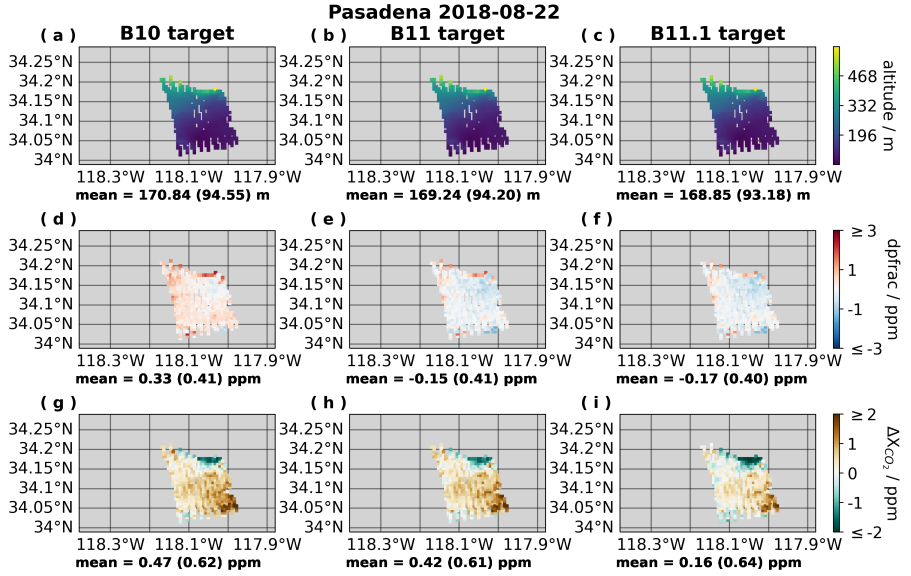

Figure S4. Sounding altitudes (top row; calculated for the sounding footprint as described in Sect. 3.1 and 3.2), retrieved dP_{frac} (middle row), and OCO-2 bias in bias-corrected X_{CO_2} relative to TCCON X_{CO_2} (see Sect. 3.3) (bottom row) during an OCO-2 target-mode overpass at Pasadena on 22 August 2018. Plots (a), (d), and (g) show results with OCO-2 v10 retrievals. Plots (b), (e), and (h) show results with OCO-2 v11 retrievals. Plots (c), (f), and (i) show results with the OCO-2 v11.1 retrievals. Only soundings that pass quality control filters in all three versions of the OCO-2 retrievals are included, such that the same set of soundings are included in all plots.

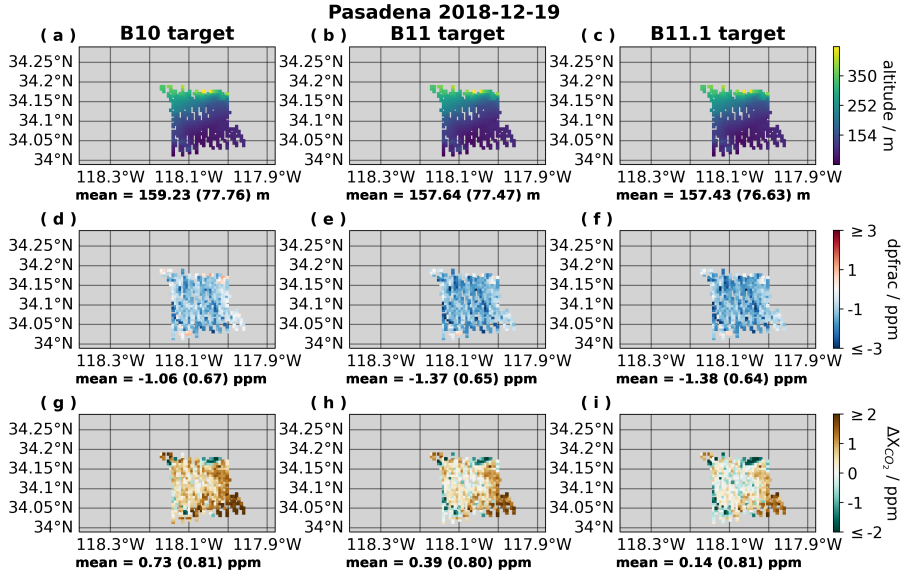

Figure S5. Sounding altitudes (top row; calculated for the sounding footprint as described in Sect. 3.1 and 3.2), retrieved dP_{frac} (middle row), and OCO-2 bias in bias-corrected X_{CO_2} relative to TCCON X_{CO_2} (see Sect. 3.3) (bottom row) during an OCO-2 target-mode overpass at Pasadena on 19 December 2018. Plots (a), (d), and (g) show results with OCO-2 v10 retrievals. Plots (b), (e), and (h) show results with OCO-2 v11 retrievals. Plots (c), (f), and (i) show results with the OCO-2 v11.1 retrievals. Only soundings that pass quality control filters in all three versions of the OCO-2 retrievals are included, such that the same set of soundings are included in all plots.

S3.2 Lauder

There were a limited number of target mode measurements over Lauder and due to the highly variable topography around the site most targets had limited spatial coverage after applying combined quality filtering for OCO-2 v10, v11, and v11.1. Figure S6 shows comparisons of altitude, dP_{frac}, and X_{CO_2} for the target with the most complete spatial coverage at Lauder and shows that the changes in altitude across versions are small (on the order of 1 m). Figure S6 also suggests that the bias in X_{CO_2} is largest (most negative) in v11.1, with the standard deviation in bias being slightly better in v11.1 than v10, but lowest in v11. On the other hand, Fig. S7 and S8 show targets with an overall reduction in mean X_{CO_2} bias in v11.1 compared to v10 or v11. This comes with the caveat that there is reduced spatial coverage for these targets.

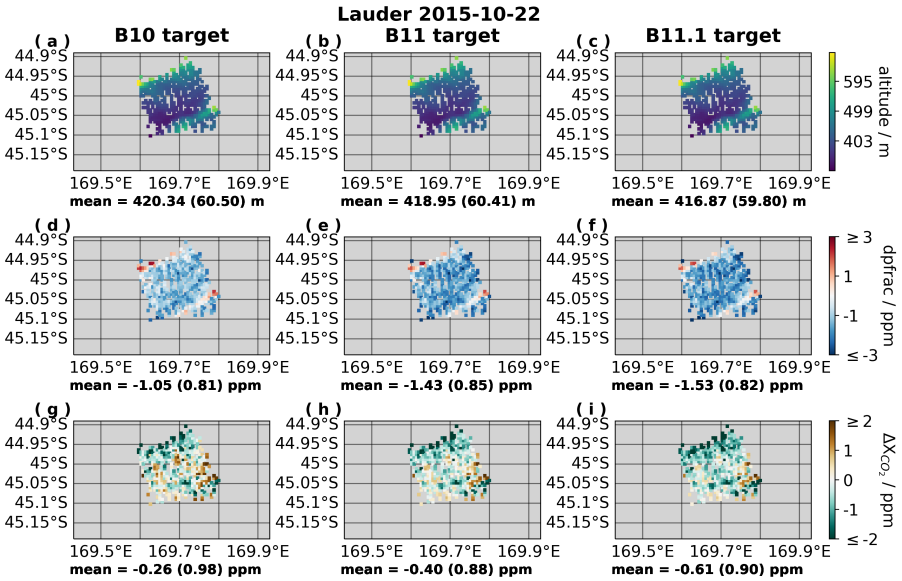

Figure S6. Sounding altitudes (top row; calculated for the sounding footprint as described in Sect. 3.1 and 3.2), retrieved dP_{frac} (middle row), and OCO-2 bias in bias-corrected X_{CO_2} relative to TCCON X_{CO_2} (see Sect. 3.3) (bottom row) during an OCO-2 target-mode overpass at Lauder on 22 October 2015. Plots (a), (d), and (g) show results with OCO-2 v10 retrievals. Plots (b), (e), and (h) show results with OCO-2 v11 retrievals. Plots (c), (f), and (i) show results with the OCO-2 v11.1 retrievals. Only soundings that pass quality control filters in all three versions of the OCO-2 retrievals are included, such that the same set of soundings are included in all plots.

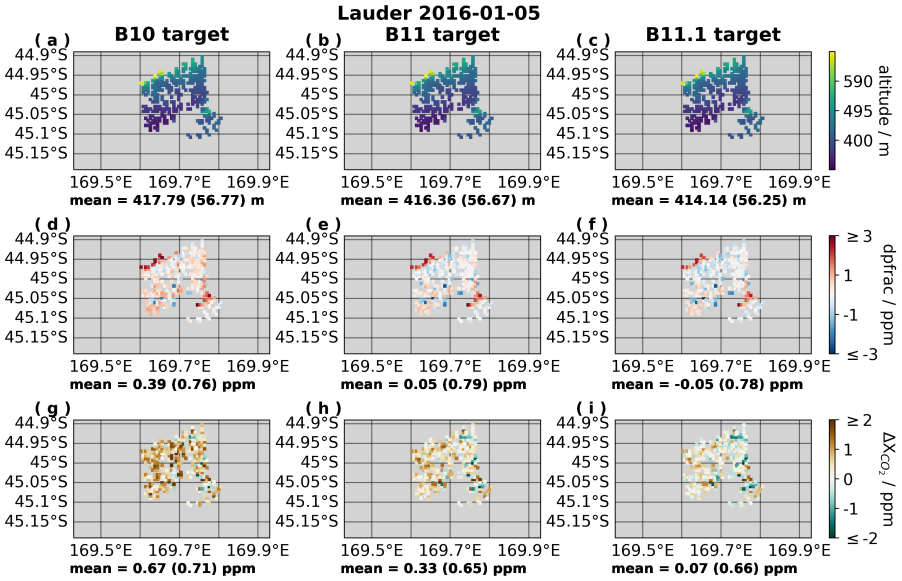

Figure S7. Sounding altitudes (top row; calculated for the sounding footprint as described in Sect. 3.1 and 3.2), retrieved dP_{frac} (middle row), and OCO-2 bias in bias-corrected X_{CO_2} relative to TCCON X_{CO_2} (see Sect. 3.3) (bottom row) during an OCO-2 target-mode overpass at Lauder on 5 January 2016. Plots (a), (d), and (g) show results with OCO-2 v10 retrievals. Plots (b), (e), and (h) show results with OCO-2 v11 retrievals. Plots (c), (f), and (i) show results with the OCO-2 v11.1 retrievals. Only soundings that pass quality control filters in all three versions of the OCO-2 retrievals are included, such that the same set of soundings are included in all plots.

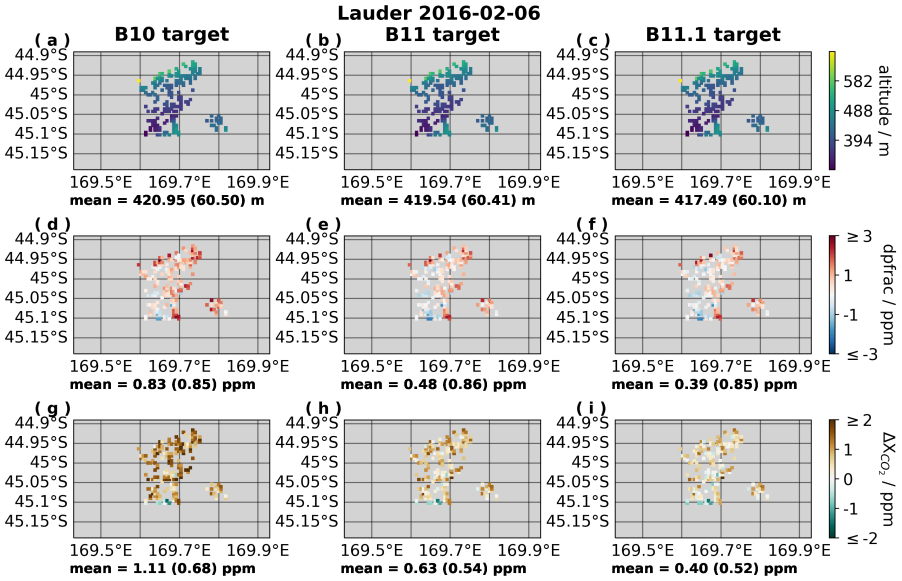

Figure S8. Sounding altitudes (top row; calculated for the sounding footprint as described in Sect. 3.1 and 3.2), retrieved dP_{frac} (middle row), and OCO-2 bias in bias-corrected X_{CO_2} relative to TCCON X_{CO_2} (see Sect. 3.3) (bottom row) during an OCO-2 target-mode overpass at Lauder on 6 February 2016. Plots (a), (d), and (g) show results with OCO-2 v10 retrievals. Plots (b), (e), and (h) show results with OCO-2 v11 retrievals. Plots (c), (f), and (i) show results with the OCO-2 v11.1 retrievals. Only soundings that pass quality control filters in all three versions of the OCO-2 retrievals are included, such that the same set of soundings are included in all plots.

S3.3 Eureka

At Eureka there are a limited number of target mode measurements and they all have sparse spatial coverage after applying all quality filtering for OCO-2 v10, v11, and v11.1. Figure S9 shows an example of a target mode measurement over Eureka with relatively favourable spatial coverage. One can see that the spatial coverage is still very sparse, possibly due in part to the rough topography around the sight. Figure S9 does suggest that there are significant differences in the sounding altitudes across OCO-2 versions with the different DEMs and, at least in this example, the mean bias in X_{CO_2} and standard deviation in bias are reduced in v11.1, relative to v10 and v11. However, it is difficult to draw conclusions when so much of the data has been screened out by quality filtering.

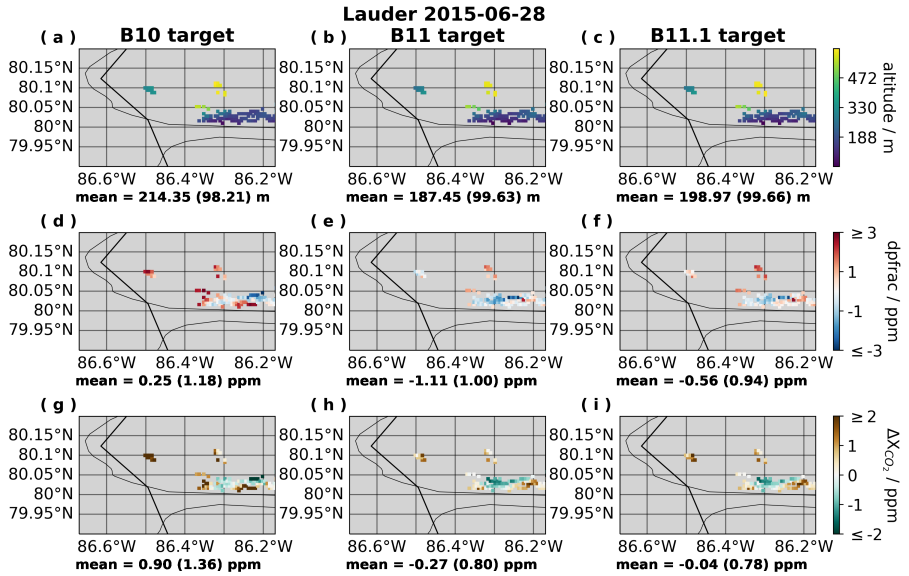

Figure S9. Sounding altitudes (top row; calculated for the sounding footprint as described in Sect. 3.1 and 3.2), retrieved dP$_{frac}$ (middle row), and OCO-2 bias in bias-corrected X$_{CO_2}$ relative to TCCON X_{CO_2} (see Sect. 3.3) (bottom row) during an OCO-2 target-mode overpass at Eureka on 28 June 2015. Plots (a), (d), and (g) show results with OCO-2 v10 retrievals. Plots (b), (e), and (h) show results with OCO-2 v11 retrievals. Plots (c), (f), and (i) show results with the OCO-2 v11.1 retrievals. Only soundings that pass quality control filters in all three versions of the OCO-2 retrievals are included, such that the same set of soundings are included in all plots.